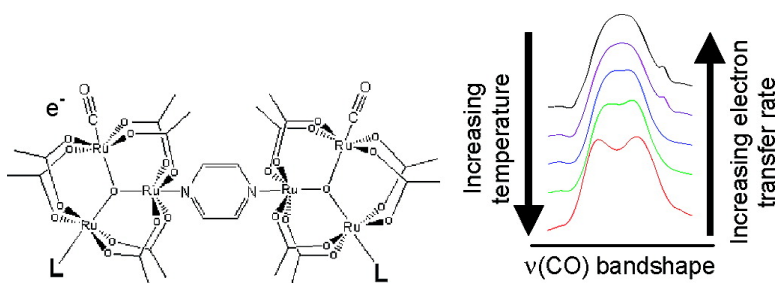


Solvent Dynamical Control of Ultrafast Ground State Electron Transfer: Implications for Class II–III Mixed Valency

Benjamin J. Lear, Starla D. Glover, J. Catherine Salsman, Casey H. Londergan, and Clifford P. Kubiak

J. Am. Chem. Soc., **2007**, 129 (42), 12772-12779 • DOI: 10.1021/ja072653m • Publication Date (Web): 29 September 2007

Downloaded from <http://pubs.acs.org> on February 14, 2009



More About This Article

Additional resources and features associated with this article are available within the HTML version:

- Supporting Information
- Links to the 2 articles that cite this article, as of the time of this article download
- Access to high resolution figures
- Links to articles and content related to this article
- Copyright permission to reproduce figures and/or text from this article

[View the Full Text HTML](#)

Solvent Dynamical Control of Ultrafast Ground State Electron Transfer: Implications for Class II–III Mixed Valency

Benjamin J. Lear, Starla D. Glover, J. Catherine Salsman, Casey H. Londergan, and Clifford P. Kubiak*

Contribution from the Department of Chemistry and Biochemistry, University of California San Diego, 9500 Gilman Drive, M/C 0358, La Jolla, California 92093-0358

Received April 16, 2007; E-mail: ckubiak@ucsd.edu

Abstract: We relate the solvent and temperature dependence of the rates of intramolecular electron transfer (ET) of mixed valence complexes of the type $\{[\text{Ru}_3\text{O}(\text{OAc})_6(\text{CO})(\text{L})_2-\text{BL}]^{-1}$, where L = pyridyl ligand and BL = pyrazine. Complexes were reduced chemically or electrochemically to obtain the mixed valence anions in seven solvents: acetonitrile, methylene chloride, dimethylformamide, tetrahydrofuran, dimethylsulfoxide, chloroform, and hexamethylphosphoramide. Rate constants for intramolecular ET were estimated by simulating the observed degree of $\nu(\text{CO})$ IR band shape coalescence in the mixed valence state. Correlations between rate constants for ET and solvent properties including static dielectric constant, optical dielectric constant, the quantity $1/\epsilon_{\text{op}} - 1/\epsilon_{\text{S}}$, microscopic solvent polarity, viscosity, cardinal rotational moments of inertia, and solvent relaxation times were examined. In the temperature study, the complexes displayed a sharp increase in the k_{et} as the freezing points of the solvents methylene chloride and acetonitrile were approached. The solvent phase transition causes a localized-to-delocalized transition in the mixed valence ions and an acceleration in the rate of ET. This is explained in terms of decoupling the slower solvent motions involved in the frequency factor ν_{N} which increases the value of ν_{N} . The observed solvent and temperature dependence of the k_{et} for these complexes is used in order to formulate a new definition for Robin–Day class II–III mixed valence compounds. Specifically, it is proposed that class II–III compounds are those for which thermodynamic properties of the solvent exert no control over k_{et} , but the dynamic properties of the solvent still influence k_{et} .

1. Introduction

Understanding the dynamics of electron-transfer reactions has been of fundamental interest to chemists, physicists, and biologists.^{1,2} Mixed valence complexes are widely known chemical systems that undergo intramolecular electron transfer. Nearly 40 years ago, Robin and Day introduced the systematic basis upon which all mixed valence complexes are classified.^{3,4} In recent years, there has been particular interest in the sometimes vague boundary between weakly localized (Class II) and fully delocalized (Class III) systems. Meyer has discussed the localized-to-delocalized transition in mixed valence chemistry and has proposed the defining characteristics of a new class, Class II–III, of mixed valence complexes.⁵ Briefly, Class II, II–III, and III systems are characterized in terms of how three types of motion — solvent, vibrational, and electronic — behave in an exchanging system. In Class II, the solvent and exchanging electron are localized. In Class II–III, the solvent is averaged and the exchanging electron is localized. In Class III, the solvent and vibrations are averaged and the exchanging electron is delocalized. Here, we report our studies of solvent dynamical

control of rates of electron transfer in mixed valence complexes in fluid and frozen solvents and consider the implications of our results with respect to the definition of Class II–III mixed valency.

The complexes of interest in this study are dimers of trinuclear ruthenium clusters containing a pyrazine bridge, Figure 1. Each triruthenium cluster contains a carbon monoxide ligand that has a distinct stretching absorption, $\nu(\text{CO})$, in the infrared (IR). Stretching frequencies of these ligands are sensitive to the electronic environment on each cluster; $\nu(\text{CO})$ bands will shift to lower frequencies in the presence of greater electron density and higher frequencies in regions of depleted electron density. In the singly reduced mixed valence state, these complexes are highly electronically coupled and undergo ground state electron transfer on the picosecond time scale. Infrared spectroscopy in the $\nu(\text{CO})$ region has proven to be a useful method to determine rate constants in the range of 10^{11} s^{-1} to 10^{13} s^{-1} by $\nu(\text{CO})$ band coalescence.⁶ This range of measurable rates is also relevant to the time scale of solvent dipolar reorientation, which, as we will show here, plays an important role in these electron-transfer reactions.

The normal rate expression for a symmetric mixed valence complex⁷ with no driving force depends on the transition

(1) Marcus, R. A. *J. Chem. Phys.* **1956**, *24*, 966–78.
(2) Hush, N. S. *Prog. Inorg. Chem.* **1967**, *8*, 391–444.
(3) Robin, M. B.; Day, P. *Adv. Inorg. Chem. Radiochem.* **1967**, *10*, 247–422.
(4) Brunshwig, B. S.; Creutz, C.; Sutin, N. *Chem. Soc. Rev.* **2002**, *31* (3), 168–184.
(5) Demadis, K. D.; Hartshorn, C. M.; Meyer, T. J. *Chem. Rev.* **2001**, *101* (9), 2655–2685.

(6) Ito, T.; Hamaguchi, T.; Nagino, H.; Yamaguchi, T.; Washington, J.; Kubiak, C. *Science* **1997**, *277* (5326), 660–663.
(7) Sutin, N. *Prog. Inorg. Chem.* **1983**, *30*, 441–98.

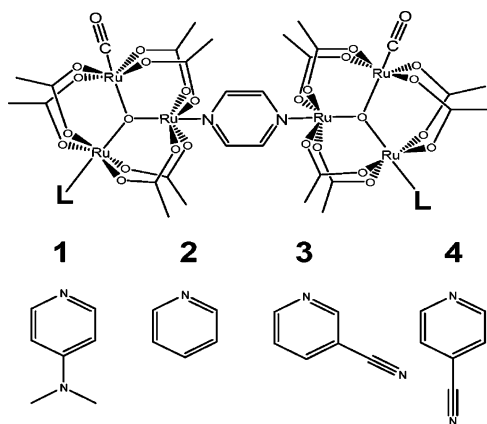


Figure 1. Structure of $[\text{Ru}_3\text{O}(\text{OAc})_6(\text{CO})(\text{L})]_2\text{-pz}$, where pz = pyrazine and ancillary ligands **1** = 4-dimethylaminopyridine (dmap), **2** = pyridine (py), **3** = 3-cyanopyridine (3-cpy), and **4** = 4-cyanopyridine (4-cpy).

probability, κ , effective nuclear frequency, ν_N , electronic coupling, H_{AB} , and thermal activation energy barrier, ΔG_λ^* .

$$k_{\text{et}} = \kappa \nu_N \exp[-(\Delta G_\lambda^* - H_{AB} + H_{AB}^2/4\Delta G_\lambda^*)/RT] \quad (1)$$

The transition probability gives the fraction of systems which, having attained the transition state, will transfer from the reactant potential energy surface to the product surface. In the adiabatic limit, $\kappa = 1$. The frequency factor, ν_N , is often described in ET reactions as the frequency at which inner sphere and outer sphere modes are in configurations required by conservation of energy for an electron to transfer from reactants to products. The thermal activation energy barrier, ΔG_λ^* , depends on the vertical reorganization energy, λ , and the electronic coupling, H_{AB} , (eq 2).⁷

$$\Delta G_\lambda^* = (\lambda - 2H_{AB})^2/4\lambda \quad (2)$$

In diabatic electron-transfer reactions, where there is no electronic coupling, $H_{AB} = 0$ and the thermal activation barrier is equal to $\lambda/4$. In the limit that the electron is totally delocalized, $H_{AB} = \lambda/2$ and the barrier for ET, ΔG_λ^* , equals zero. Thus, for complexes that are not fully delocalized, ΔG_λ^* (and therefore k_{et}) should show a dependence on the reorganization energy, λ . The reorganization energy is a sum of inner sphere and outer sphere contributions.⁷

$$\lambda = \lambda_o + \lambda_i \quad (3)$$

λ_i depends on molecular vibrations, the amount of energy required for the nuclear coordinates to rearrange following light-induced ET. λ_o , the outer sphere reorganization energy of the ET complex, includes the properties of the solvent. λ_o is determined by the optical and static dielectric constants of the solvent, ϵ_{op} and ϵ_s , in the Marcus dielectric continuum model and accounts for the energetics of the solvent nuclear rearrangement upon ET.⁷ For localized systems, λ_o will vary as a function of $(1/\epsilon_{\text{op}} - 1/\epsilon_s)$. When mixed valence complexes approach complete delocalization (Robin–Day class III), the solvent dependence of the total reorganization energy disappears due to averaging of solvent environments.

The rate of ET depends also on ν_N , the pre-exponential “frequency factor”, which is a weighted average of nuclear

frequencies for all modes that contribute to the electron-transfer reorganization energy.

$$\nu_N = \left[\sum_i \nu_i^2 E_i / \sum_i E_i \right]^{1/2} \quad (4)$$

For intramolecular ET reactions in solution these modes include solvent frequencies and intramolecular vibrations that promote ET.⁸ For Class II mixed valence ions, the exponential terms govern the rate expression (eq 1). These exponential terms, λ and H_{AB} , are generally considered to be time-independent. As H_{AB} assumes values approaching $\lambda/2$, the exponential term in eq 1 moves toward unity and the time-dependent pre-exponential terms are expected to govern the rate.

The dynamics of the solvent are included in ν_N , and the importance of solvent dipolar reorientation times on k_{et} was reported in a previous study, where it was demonstrated that k_{et}^{-1} 's scale linearly with the t_{1e} 's determined by Maroncelli and co-workers and not with normal (time-independent) solvent reorganization.^{9,10} Here, we provide further evidence that the mixed valence ruthenium dimers are controlled by the dynamics of the solvent and not the energetic properties of the solvent. We also provide a more thorough explanation of this dynamic dependence. Building upon this, we discuss the behavior of k_{et} as the solvent proceeds through the liquid to solid state transition. We end with a comment on the implications that these results have for the definition of class II–III mixed valency.

2. Experimental Section

Complexes used in this study were of the type $[\text{Ru}_3\text{O}(\text{OAc})_6(\text{CO})(\text{L})]_2\text{-}\mu\text{-pz}$ where pz = pyrazine with ancillary ligands **1** = 4-dimethylaminopyridine, **2** = pyridine, **3** = 3-cyanopyridine, and **4** = 4-cyanopyridine, Figure 1. Complexes **1–4** were prepared as described previously.¹¹ Complex **5**, $\text{Ru}_3\text{O}(\text{OAc})_6(\text{CO})(4\text{-cpy})_2$, was obtained as a side product during the synthesis of complex **4**.

The solvents for this study were chosen such that the mixed valence state of the complex is soluble and is stable over a wide range of temperatures. For the optical cryostat studies, acetonitrile and methylene chloride were dried over basic alumina with a custom dry solvent system. Solutions (10 mM) of each dimer were chemically reduced to the mixed valence state with 1.1 molar equiv of cobaltocene ($E^\circ = -1.33$ V vs Fc/Fc⁺)¹² in an inert atmosphere. Spectra of mixed valence dimers were recorded on a Bruker Equinox 55 FTIR in a flow through an optical cryostat (Specac, model number 21525). The sample cell, consisting of CaF₂ windows with a path length of 0.1 mm, is contained in a vacuum jacketed housing. Addition of liquid nitrogen to the cooling compartment followed by heating to the desired temperature with a computer-controlled thermocouple/heating coil regulates temperature in the sample cell. Solvents for use in IR spectroelectrochemistry were dried and distilled by the usual methods. The IR spectroelectrochemical responses were measured in a sixth-generation home-built cell mounted onto a specular reflectance unit. The cell has been described in detail elsewhere.¹³ Simulation of IR spectra to estimate ET rate constants was performed with VibexGL, a program for the simulation of IR spectra of exchanging systems.¹⁴

- (8) Weaver, M. J. *Chem. Rev.* **1992**, 92 (3), 463–80.
- (9) Horng, M. L.; Gardecki, J. A.; Papazyan, A.; Maroncelli, M. *J. Phys. Chem.* **1995**, 99 (48), 17311–37.
- (10) Londergan, C. H.; Salsman, J. C.; Ronco, S.; Dolcas, L. M.; Kubiak, C. P. *J. Am. Chem. Soc.* **2002**, 124 (22), 6236–6237.
- (11) Kido, H.; Nagino, H.; Ito, T. *Chem. Lett.* **1996**, 25 (9), 745–746.
- (12) Connelly, N. G.; Geiger, W. E. *Chem. Rev.* **1996**, 96 (2), 877–910.
- (13) Zavarine, I. S.; Kubiak, C. P. *J. Electroanal. Chem.* **2001**, 495 (2), 106–109.
- (14) McClung, R. E. D. *VibexGL: Program for the Simulation of IR Spectra of Exchanging Systems*.

Table 1. k_{et}^{-1} for Complexes 1–4 at $-30\text{ }^{\circ}\text{C}$ and Selected Solvent Thermodynamic Parameters

solvent	1 k_{et}^{-1} / ps	2 k_{et}^{-1} / ps	3 k_{et}^{-1} / ps	4 k_{et}^{-1} / ps	ϵ_s^a	ϵ_{op}^b	$(1/\epsilon_{\text{op}} - 1/\epsilon_s)$	E_T^c / kcal mol $^{-1}$
CH ₃ CN	0.35(5)	0.38(5)	0.72(10)	0.91(12)	35.94	1.81	0.526	45.6
CH ₂ Cl ₂	0.50(5)	0.57(5)	0.72(12)	0.91(11)	8.93	2.03	0.381	40.7
DMF	0.67(12)	0.77(15)	0.91(10)	1.0(2)	36.71	2.04	0.462	43.2
THF	0.83(15)	0.95(15)	1.0(1)	1.0(1)	7.58	1.98	0.373	37.4
DMSO	0.77(10)	0.87(14)	1.1(1)	0.9(1)	46.45	2.19	0.435	45.1
CHCl ₃	1.5(2)	1.8(2)	1.9(1)	2.0(1)	4.81	2.09	0.270	39.1
HMPA	1.5(2)	2.2(2)	2.5(5)	3.3(3)	29.30	2.13	0.436	40.9
$R^{2,d}$	--	--	--	--	0.040	0.280	0.191	0.169

^a Values for the static dielectric constants were obtained from ref 15. ^b Values for the optical dielectric constants were obtained by squaring the refractive index of the solution. Values for the refractive index were obtained from ref 15. ^c The microscopic polarity of the solvents was obtained from ref 15. ^d R^2 terms were obtained from a linear regression fit to a plot of k_{et}^{-1} versus the solvent parameter for each of the complexes 1–4 and was then averaged over all the complexes.

Table 2. k_{et}^{-1} for Complexes 1–4 Obtained at $-30\text{ }^{\circ}\text{C}$ and Selected Solvent Dynamic Parameters

solvent	1 k_{et}^{-1} / ps	2 k_{et}^{-1} / ps	3 k_{et}^{-1} / ps	4 k_{et}^{-1} / ps	η^g / 10 $^{-3}$ Pa s	I_x^h / g Å 2 mol $^{-1}$	I_y^h / g Å 2 mol $^{-1}$	I_z^h / g Å 2 mol $^{-1}$	τ_o^i / ps	$\langle\tau\rangle^j$ / ps	t_{1e}^k / ps
CH ₃ CN	0.35(5)	0.38(5)	0.72(10)	0.91(12)	0.345	3.31	55.53	55.54	0.12	0.26	0.15
CH ₂ Cl ₂	0.50(5)	0.57(5)	0.72(12)	0.91(11)	0.441	16.2	156.9	169.7	0.25	0.56	0.38
DMF	0.67(12)	0.77(15)	0.91(10)	1.0(2)	0.924	56.8	122.8	172.9	0.38	2	0.67
THF	0.83(15)	0.95(15)	1.0(1)	1.0(1)	0.575	70.5	72.2	125.3	0.43	0.94	0.7
DMSO	0.77(10)	0.87(14)	1.1(1)	0.9(1)	1.991	72.3	73.4	120.5	0.4	2	0.9
CHCl ₃	1.5(2)	1.8(2)	1.9(1)	2.0(1)	0.058	152.83	152.96	295.2	0.71	2.8	2.3
HMPA	1.5(2)	2.2(2)	2.5(2)	3.3(3)	3.47	474	580	712	0.3	9.9	5.9
$R^{2,d}$	--	--	--	--	0.334	0.825	0.657	0.748	0.234	0.764	0.860

^a Values for solvent viscosities were obtained from ref 15. ^b Values for the principal moment of inertia were calculated using ChemDraw 3D. ^c The solvent dynamic parameters, τ_o , $\langle\tau\rangle$, and t_{1e} were obtained from ref 9. ^d R^2 terms were obtained from a linear regression fit to a plot of k_{et}^{-1} versus the solvent parameter for each of the complexes 1–4 and was then averaged over all the complexes.

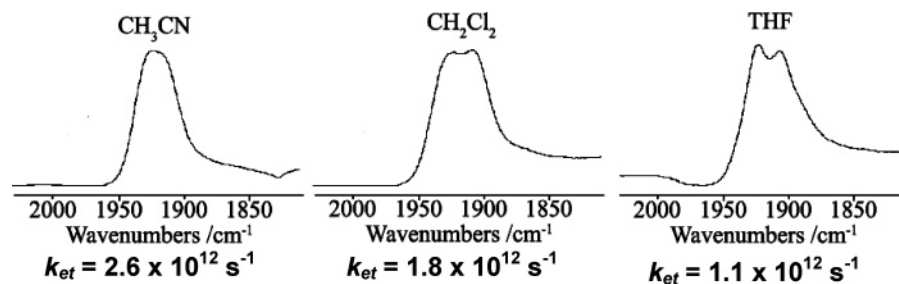


Figure 2. IR band shapes for the $\nu(\text{CO})$ band of 2^- in CH₃CN, CH₂Cl₂, and THF. The estimated electron-transfer rate (k_{et}) is given below the spectra. More coalesced spectra are associated with faster electron-transfer rates.

3. Results and Discussion

3.1. Solvent Effects on Electron-Transfer Rates. This report follows an earlier study of the solvent dependence of the electron-transfer rates in complexes 1–4.¹⁰ Here, we present a more complete discussion of the effects of solvent upon the observed electron-transfer rate constants, k_{et} , of these complexes. Tables 1 and 2 present measured values of k_{et}^{-1} for complexes 1–4 in acetonitrile, methylene chloride, dimethylformamide, tetrahydrofuran, dimethyl sulfoxide, chloroform, and hexamethylphosphoramide. Figure 2 shows $\nu(\text{CO})$ bands of 2^- in acetonitrile, chloroform, and tetrahydrofuran with the rate constants estimated from band shape simulation. It is clear from the data that more coalesced band shapes correspond to faster rate constants. Additionally, Table 1 lists solvent parameters that reflect the time-independent energetic properties of these solvents, while Table 2 contains parameters that reflect the time-dependent dynamical properties of these solvents. The energetic parameters are the outer sphere reorganization energy (λ_o), the optical and static dielectric constants (ϵ_{op} and ϵ_s), and the solvent microscopic polarity (E_T).¹⁵ The dynamic parameters are

the solvent viscosity (η), the principle moments of inertia (I_x , I_y , and I_z), and solvent relaxation parameters as defined by Maroncelli and co-workers (τ_o , $\langle\tau\rangle$, and t_{1e}). At the bottom of the columns associated with the solvent parameters is an average R^2 value. This R^2 term was obtained from a linear regression fit to a plot of k_{et}^{-1} versus the relevant solvent parameter for each of the complexes 1–4 and was then averaged over all four of the complexes. The R^2 values are provided to help the reader quickly evaluate the degree of correlation between k_{et}^{-1} and the various solvent parameters. The quantity k_{et}^{-1} is used instead of k_{et} since most of the dynamic solvent parameters are expressed as lifetimes. Higher R^2 values indicate a stronger correlation between k_{et}^{-1} and the parameter of interest. Using the data gathered in Tables 1 and 2, we can begin to discuss the role that solvent plays in highly coupled mixed valence systems undergoing ultrafast electron transfer.

3.2. Electron-Transfer Rate Dependence on Time-Independent Solvent Parameters. The first parameter to be addressed is the outer-sphere reorganizational energy (λ_o), which

(15) Stephen L.; Murov, I. C.; Hug, G. L. *Handbook of Photochemistry*, 2nd ed.; Marcel Dekker, Inc.: 1993.

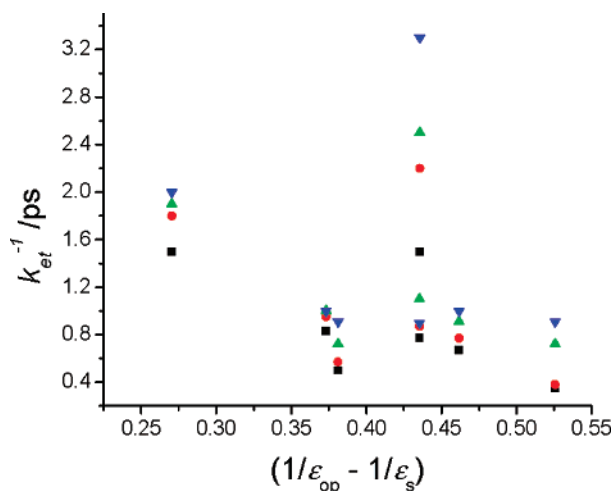


Figure 3. Plot $(1/\epsilon_{\text{op}} - 1/\epsilon_{\text{s}})$ — the variable portion of the outer sphere reorganization energy, λ_{o} — versus the lifetime for electron transfer, k_{et}^{-1} , for complexes **1** (■), **2** (●), **3** (▲), and **4** (▼). The average of the R^2 values for this plot is 0.191.

is a measure of the energetic contributions of the solvent to the barrier for instantaneous (optically induced) electron transfer.⁷

$$\lambda_{\text{o}} = \frac{(\Delta e)^2}{8\pi} \left(\frac{1}{\epsilon_{\text{op}}} - \frac{1}{\epsilon_{\text{s}}} \right) \int (D_{\text{A}} - D_{\text{B}})^2 d\tau \quad (5)$$

Here, Δe is the charge transferred, ϵ_{op} is the optical dielectric constant, ϵ_{s} is the static dielectric constant, and D_{A} and D_{B} are the dielectric displacement vectors of the precursor and successor complexes, respectively. For electron transfer in a given system in different solvents, Δe^2 , D_{A} , and D_{B} remain unchanged. The changes to λ_{o} brought about through changes in solvent are accounted for by the term $(\epsilon_{\text{op}}^{-1} - \epsilon_{\text{s}}^{-1})$. The parameter λ_{o} is included in the expression for the barrier to thermal electron transfer (activation energy) as given by eq 1, and the term $(\epsilon_{\text{op}}^{-1} - \epsilon_{\text{s}}^{-1})$ normally shows good correlation with the observed electron-transfer rates for mixed valence complexes. We expected this to be true for **1–4**, but this is not the case. Figure 3 is a plot of $(\epsilon_{\text{op}}^{-1} - \epsilon_{\text{s}}^{-1})$ versus k_{et}^{-1} . Examination of Figure 3 shows that there is no correlation between λ_{o} and k_{et}^{-1} . This is surprising, but the data are clear; λ_{o} does not capture the solvent dependence of the mixed valence ions **1–4**. In this important respect, **1–4** are behaving as if they were class III systems.

Although λ_{o} and k_{et}^{-1} are not correlated, it is possible that a single dielectric constant could capture the solvent dependence of complexes **1–4**. The static dielectric constant, ϵ_{s} , is a measure of the solvent response to an applied electric field, gauging the extent to which the solvent is affected by the external field. It is given by the following equation.¹⁶

$$\epsilon_{\text{s}} = \frac{4\pi}{3} N_{\text{o}} \left(\alpha_{\text{o}} + \frac{\mu^2}{3kT} \right) \quad (6)$$

Here, α_{o} is the polarizability of the solvent molecules, which accounts for how their electron clouds are deformed by local electric fields, and the μ term accounts for the orientation of the permanent dipole moment of the solvent in response to an

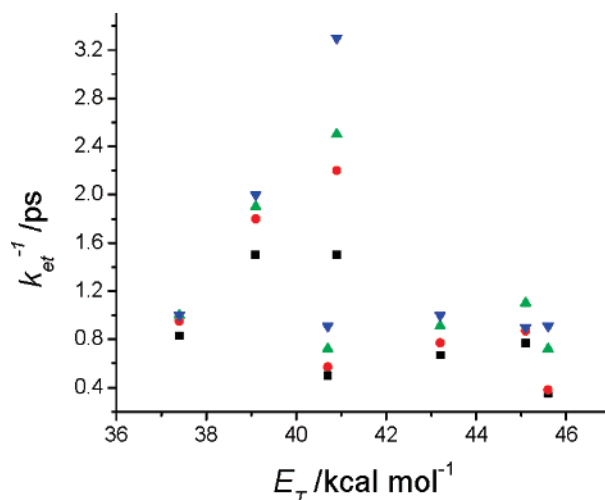


Figure 4. Plot of the microscopic polarity of the solvent, E_{T} , versus the lifetime for electron transfer, k_{et}^{-1} , for complexes **1** (■), **2** (●), **3** (▲), and **4** (▼). The average of the R^2 values for this plot is 0.169.

applied field. Thus, ϵ_{s} should provide a parameter for how the solvent responds to the change in dipole moment that occurs upon electron transfer. However, ϵ_{s} only describes the solvent's response when the applied field is either static or oscillates at frequencies less than that associated with the far IR (10^{11} s^{-1}). At oscillations in the field that have frequencies greater than that associated with far IR the orientational term (μ) in eq 2 drops out, as the solvent can no longer keep pace with the changes in the electric field. The dielectric constant that results from the exclusion of the orientational term is termed the optical dielectric (ϵ_{op}) and is equal to the square of the refractive index of the solvent, n^2 .¹⁶ The ET rates measured for **1–4** are on the order of 10^{11} s^{-1} , and because of this, it is not surprising that k_{et}^{-1} and ϵ_{s} show no correlation (Table 1). Because the ET rate is fast, ϵ_{op} is expected to be a better parameter for comparison with k_{et} . However, as can be found in Table 1, the correlation between ϵ_{op} and k_{et}^{-1} remains quite poor. It should be noted that even though there is some frequency dependence of the dielectric constants, they remain static parameters (they account for the magnitude of the solvent response to the applied field and not the dynamics of this response). In any case, it is easily seen that no clear correlation exists between the dielectric constants of solvents and k_{et}^{-1} .

Despite the fact that λ_{o} , ϵ_{op} , and ϵ_{s} have failed to explain the solvent dependence exhibited by complexes **1–4**, it is difficult to depart from the assumption that the major contribution to the rate of electron transfer will stem from the reorganization of the solvent's nuclear coordinates following the shift in charge associated with electron transfer. Thus, we consider another parameter that may capture this contribution. A logical conjecture is that the electron transfer correlates with solvent polarity. Clearly, the polarity of the solvent should reflect the strength of the response of the solvent to a change in charge distribution following an electron-transfer event. This response to a change in the local electronic environment could be accounted for by the microscopic polarity (E_{T}) of the solvent. However, Figure 4 (a plot of k_{et}^{-1} versus E_{T}) shows that ET rates in our complexes do not depend on solvent polarity.

Up to this point it has been shown that there is no good correlation between k_{et}^{-1} and λ_{out} , ϵ_{op} , ϵ_{s} , or E_{T} . Thus, there appears to be no connection between the strength of solvent

(16) Shoemaker, D. P.; Garland, C. W. *Experiments in Physical Chemistry*, 2nd ed.; McGraw-Hill: New York, 1962; p 490.

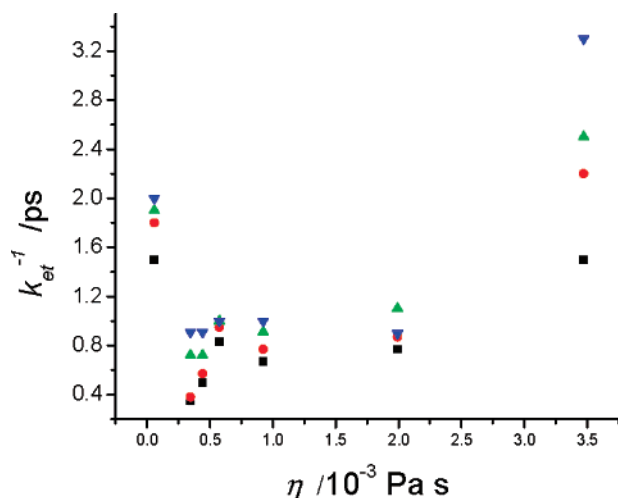


Figure 5. Plot of solvent viscosity, η , versus the lifetime for electron transfer, k_{et}^{-1} , for complexes **1** (■), **2** (●), **3** (▲), and **4** (▼). The average of the R^2 values for this plot is 0.334.

response and changes in the local fluctuating electric field around **1–4**. That is, the energetics of the solvent's response to changes in electric dipole seem to have no influence on k_{et} . Reference to eq 1 suggests the boundary conditions for this type of behavior to be observed.

For strongly coupled systems ($H_{AB} = \lambda/2$) the exponential term will be close to zero and the value of the exponential approaches unity. For nearly activationless electron transfer, it is the pre-exponential term (ν_N) that will dominate the expression for k_{et} . The pre-exponential term is the weighted average of all internal vibrational modes that contribute to electron transfer and nuclear reorganization *as well as* the solvent modes that allow for reorganization of the solvent following the ET event. We see why normal assumptions about solvent reorganization fail to capture the solvent dependence of **1–4**. The parameters λ_o , ϵ_{op} , ϵ_s , and E_T all quantify different time-independent thermodynamics of the solvent contribution, which, when the value of the exponential term is *not* near zero, have a large impact on the electron-transfer rate. However, in the highly coupled case when the exponential approaches unity, the pre-exponential frequencies control the rates of ET. We therefore turn our attention away from the static thermodynamic properties of the solvents and toward the *dynamic* properties of the solvents.

3.3. Electron-Transfer Rate Dependence on Time-Dependent Solvent Parameters. A simple solvent parameter that we can use as a metric for solvent dynamics important in fluidity is the solvent viscosity, η . Viscosity is a function of the rate at which a fluid's velocity changes over distance (dv/dx) and, as such, is a measure of the restriction of translational motion. In polar solvents with more restricted motion, it is expected that ν_N and, as a result of this, k_{et} will decrease in value. This general trend is observed in Figure 5, which is a plot of solvent viscosity versus k_{et}^{-1} . While the correlation between these two parameters is by no means excellent, it is vastly improved over those found in Figures 3 and 4 and provides a satisfying agreement with the intuitive reasoning presented above. The poor correlation most likely stems from the fact that while there is certainly some degree of translational motion of the solvent in response to the ET, it seems more likely that the major reorganizational movement is that of rotation of the dipole. That is, following

the change in the charge distribution associated with ET the solvent needs to rotate such that its dipole moment is correctly oriented with respect to this new charge distribution. Indeed, this picture is supported by work done by Stratt and co-workers.^{17,18} Simulation and analysis of solvation spectra for dipolar solutes in polar solvents showed that the rotational rearrangement of the solvent molecules accounts for the major contributions to solvation of the solutes as well as the observed timescales of solvation. In contrast, they found that translational motion of solvation is largely universal among differing solvents and did not account for the observed differences in the time scale of solvation. This supports the idea that differences in the dynamics of solvent (and the effects that these dynamics will have on the overall dynamics of a system) are largely a result of rotational motion of the solvent. Relying on the assumption that rotational motions are the most important for initial solvent reorganization, Weaver has derived an expression for ν_N that depends solely on the rotational motion of the solvent.⁸

$$\nu_N = (2\pi\tau_{\text{rot}})^{-1} \quad (7)$$

Here, τ_{rot} is termed the “solvent-phase inertial rotation time.” This parameter attempts to explain the rotation of molecules within a dielectric medium. While rotational motion probably plays into the physical property of viscosity (one expects that as viscosity increases the rotational motion of the molecules will be somewhat inhibited), it should be a minor contribution. Thus, it would be useful to find a new parameter that can more accurately predict the rotational motion of the solvent. The term τ_{rot} should correlate with the electron-transfer rates. This parameter, however, is not straightforward to obtain for all solvents in our study. We turn instead to simpler parameters that quantitatively address the rotational motions of the solvent, namely the principal moments of rotational inertia.

The rotational moments of inertia (**I**) for solvent molecules can be calculated using commercial software¹⁹ and are expected to provide a useful measure of the ease of dipole reorientation. Clearly, the rate of rotation is inversely proportional to the rotational inertia of the solvent molecules. Because the rate of electron transfer is controlled by the dynamics of the solvent and the rotational reorientation of the solvent dipole is required to accommodate the movement of the electron, we expect to find a strong correlation between the moments of inertia of the solvent and the electron-transfer rates of complexes **1–4**. Examination of Table 2 shows that **I_x**, **I_y**, and **I_z** all have good correlations with k_{et}^{-1} . However, **I_x** shows the strongest correlation. A plot of **I_x** versus k_{et}^{-1} is shown in Figure 6 in order to demonstrate the trend. **I_x** is defined as the smallest principal moment of inertia, and as such, rotation along this axis is expected to be easiest. To a first approximation, rotation of the solvent by exerting a force resulting from the change in an external dipole should be principally about the “easy” axis (the axis with the lowest rotational moment of inertia). Thus, it is quite satisfying that **I_x** shows the strongest correlation with k_{et}^{-1} .

The case of acetonitrile deserves comment, especially the correlation of **I_x** with k_{et}^{-1} . Acetonitrile is a linear molecule, and as such, rotation along the defined *x*-axis is rotation along the long axis of the molecule and is not expected to change the

(17) Stratt, R. M.; Maroncelli, M. *J. Phys. Chem.* **1996**, *100* (31), 12981–12996.

(18) Stratt, R. M. *Acc. Chem. Res.* **1995**, *28* (5), 201–7.

(19) CambridgeSoft *CS Chem3D Ultra*, 7.0.0; CambridgeSoft: 2001.

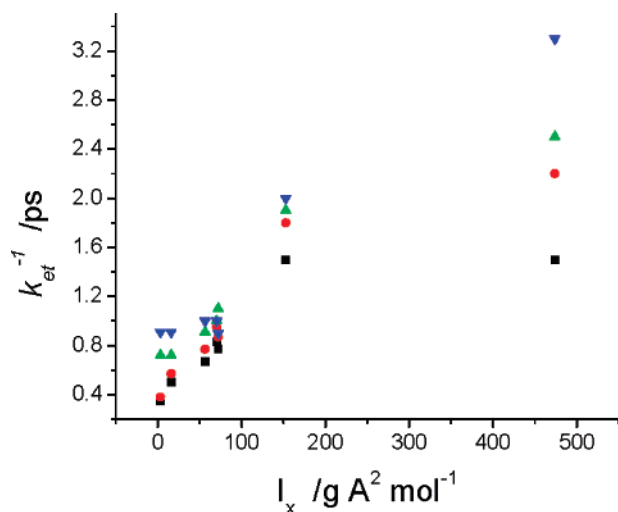


Figure 6. Plot of the moment of inertia along the solvent's x -axis, I_x , versus the lifetime for electron transfer, k_{et}^{-1} , for complexes **1** (■), **2** (●), **3** (▲), and **4** (▼). The average of the R^2 values for this plot is 0.825.

orientation of the dipole moment. Thus, it could be questioned whether it is valid to include I_x when considering the reorientation of acetonitrile. While it is true that acetonitrile is linear, this is only the static, lowest energy conformation. Vibrational bending motions of the molecule, of course, distort it from linearity. In such a distorted geometry, rotations along the x -axis do reorient the dipole. One can also consider the correlation that results when I_y is substituted for I_x for acetonitrile in Figure 6. In this case, the average R^2 value is 0.792, which is still a better correlation than that for any parameter other than I_x . The key point is that it is the inertial properties of all solvents studied that are most strongly correlated with k_{et}^{-1} , and this underscores the importance of solvent rotational motion in the electron-transfer process.

It is clear from Figures 3–6 as well as the data presented in Tables 1 and 2 that k_{et} is affected by the dynamics of the solvent. However, the moments of inertia only account for rotation of the solvent. While rotation should play the major role in the reorganization of the solvent, translational modes are most certainly involved. Translational movement is required for the solvent to realize the geometric coordinates that minimize the potential energy resulting from the interaction of their dipoles with the mixed-valence system. Thus, it would be useful to compare k_{et}^{-1} with parameters that take into account both the rotational and translational motions of the solvent in response to the movement of charge. Maroncelli's experimental work on solvent relaxation dynamics has provided these parameters.⁹ The work by Maroncelli and co-workers is the most comprehensive on solvent relaxation to date. This group measured the time-resolved multiexponential Stokes shift in the fluorescence of Coumarin 153 in a wide range of solvents. The fastest responses were attributed to solvent rotational motion. This motion is ascribed to the reorientation of the solvent dipole in order to stabilize the new charge distribution in excited Coumarin 153. The slower times were attributed to translational motion to attain the most stabilized excited state. Maroncelli calculated three characteristic solvent relaxation times for most common solvents. The first, τ_0 , is the instantaneous response before solvent motion evolves. It deals with exceptionally fast time scales. The second, $\langle\tau\rangle$, is the average lifetime of all

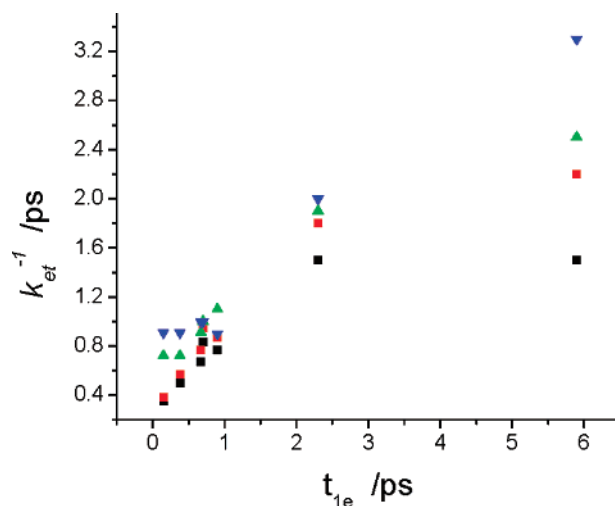


Figure 7. Plot of the characteristic solvent relaxation time, t_{1e} , versus the lifetime for electron transfer, k_{et}^{-1} , for complexes **1** (■), **2** (●), **3** (▲), and **4** (▼). The average of the R^2 values for this plot is 0.860.

components observed in the solvent response and accounts for the behavior of the solvent over long time periods. The third, t_{1e} , is the time required for the solvent response function to reach $1/e$ and may be thought of as encompassing the total evolution of the solvent dynamic response to changes in the local electronic environment. Of these three parameters, τ_0 clearly shows the worst correlation with k_{et}^{-1} while t_{1e} provides the best (k_{et}^{-1} versus t_{1e} is plotted in Figure 7). This is not wholly unexpected. The parameter τ_0 deals with the time before the solvent motion gets underway and may be considered an instantaneous polarizability. These are not expected to contribute significantly to the attainment of the transition state and, hence, to the value of ν_N . The values of $\langle\tau\rangle$ are, in general, slower than our measured ET rates and, as a result, were not expected to be strongly correlated with k_{et}^{-1} . The fact that $\langle\tau\rangle$ does show good correlation with k_{et}^{-1} may indicate that slower solvent motions need to be included in the total solvent response to ET in **1–4**. Finally, t_{1e} as a parameter enveloping the full range of solvent dynamics provides the best correlation to k_{et}^{-1} of the solvent parameters we have explored. This is very reasonable if the total ensemble response of the solvent is to be considered when investigating the solvent dependence of ultrafast electron transfer.

Referring back to Tables 1 and 2, we are now prepared to make a few comments on the general trends that emerge in the correlation between k_{et}^{-1} and solvent parameters. First, it is clear that there are poor correlations between k_{et}^{-1} and solvent parameters that are mostly thermodynamic in nature (such as λ_o , ϵ_{op} , and ϵ_s). Second, parameters (such as I_x and t_{1e}) that address important dynamic solvent properties show good correlations with k_{et}^{-1} . The solvent parameters that show the strongest correlations with k_{et}^{-1} are ones that correspond to the fast movement of solvent in response to an external force (change in dipole). These parameters are I_x and t_{1e} , and they show an extremely similar correlation, suggesting that they address very similar dynamical processes of the solvent.

Given the form of eq 1 and the fact that solvent thermodynamic parameters provide poor correlation with observed k_{et}^{-1} while solvent dynamics provide excellent correlation with observed k_{et}^{-1} , it seems justified to assume that it is the solvent dynamics that are controlling the electron-transfer rates of

complexes **1–4** via the pre-exponential term. This pre-exponential control is a result of the fact that the solvent modes are included in the pre-exponential term and the fact that the electronic coupling, H_{AB} , in these complexes is large enough (approaching $\lambda/2$) that the value of the exponential approaches unity and the rate of electron transfer should be controlled by the value of ν_N .

As seen in eq 2, ν_N contains contributions from solvent modes and Weaver's derivation of ν_N in eq 7 seems to indicate that the solvent dynamics are expected to be major contributors to ν_N in fluid solution. However, the solvent dynamics are expected to be much slower than the internal vibrational modes of the molecule that contribute to ET. For comparison, it is known that the ν_{8a} mode of the bridging pyrazine is strongly coupled to the ET event in these complexes²⁰ and, therefore, should be figured into the pre-exponential term. The frequency of this vibration is $4.8 \times 10^{13} \text{ s}^{-1}$ while the relaxation "frequency" of even the fastest solvent we have used (acetonitrile) is $6.7 \times 10^{12} \text{ s}^{-1}$ (using t_{1e}). Clearly the relaxation of the solvent is a process that limits the electron-transfer rate of the complexes. Thus, if it were possible to decouple the solvent dynamics from the electron-transfer event, we would remove the "solvent friction" from the system and increase the overall ET rate.

3.4. Decoupling of Solvent Modes from Rates of Electron Transfer. It has been predicted that the decoupling of the solvent modes from the electron-transfer rate may be achieved by freezing the solvent in which the electron transfer is occurring.²¹ The main effect of this decoupling is that solvent dipolar reorientation will no longer play a dynamic role in the reorganization of the system and ν_N will consist only of a weighted average of intramolecular vibrations. When solvent friction is removed, the pre-exponential is expected to increase from 10^{12} s^{-1} to 10^{13} s^{-1} . The interesting and counterintuitive result that must follow from this is that the rate of electron transfer is expected to increase as the solvent temperature decreases. However, this increase in rate should only occur near the freezing point of each solvent and then change no further (i.e., solvent modes decouple once frozen and remain uncoupled). Using **1**, **2**, and **4** in methylene chloride (mp = $-92 \text{ }^\circ\text{C}$) and acetonitrile (mp = $-44 \text{ }^\circ\text{C}$), FTIR spectra were collected from $25 \text{ }^\circ\text{C}$ to the freezing point and below for each solvent. In all cases, as the temperature of the system was decreased from $25 \text{ }^\circ\text{C}$ to just above the freezing point of the solvent, non-Arrhenius behavior of the electron-transfer rate was observed (a slight increase in estimated rate constants occurred at lower temperatures). This is consistent with very low barriers to ET. As the freezing point of the solvent was approached, a dramatic increase in the $\nu(\text{CO})$ coalescence occurred. Lowering the temperature past the freezing point of the solvent resulted in no further coalescence or change in the IR spectra. Figures 8 and 9 show **4** in methylene chloride and acetonitrile, respectively. It is clear that as the solvent freezes, the $\nu(\text{CO})$ band shape coalesces and that beyond the freezing point of the solvent no further coalescence was observed. Complex **4**, which has the slowest exchange rate of **1–4**, shows the most dramatic change in coalescence. Complexes **1** and **2**, which show more coalesced $\nu(\text{CO})$ spectra at $25 \text{ }^\circ\text{C}$ compared to **4**'s do not show as striking an increase in the band shape coalescence. Tables 3

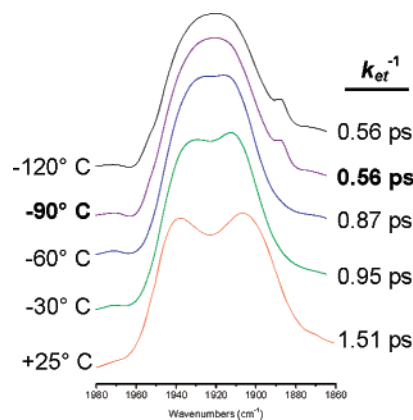


Figure 8. IR band shape for $\nu(\text{CO})$ of the mixed valence dimer **4** in CH_2Cl_2 as a function of temperature. The band shape shows increasing coalescence as the freezing point of the solution is approached (ca. $-92 \text{ }^\circ\text{C}$). To the right of each spectrum are listed the electron-transfer lifetimes obtained from simulation of that spectrum.

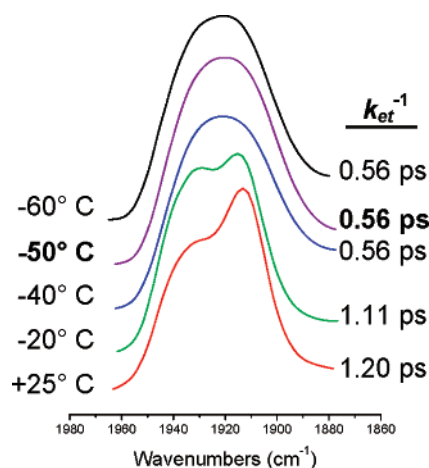


Figure 9. IR band shape for $\nu(\text{CO})$ of the mixed valence dimer **4** in CH_3CN as a function of temperature. The band shape shows increasing coalescence as the freezing point of the solution is approached (ca. $-44 \text{ }^\circ\text{C}$). To the right of each spectrum are listed the electron-transfer lifetimes obtained from simulation of that spectrum.

Table 3. k_{et}^{-1a} for Complexes **1**, **2**, and **4** in CH_2Cl_2

	temperature/ $^\circ\text{C}$				
	25	-40	-60	-80	-90
1	0.50	0.50	0.43	0.43	0.29
2	0.74	0.56	0.56	0.48	0.40
4	1.52	0.95	0.87	0.71	0.56

^a Values of k_{et}^{-1} are given in units of ps. Uncertainties are 0.02 ps.

Table 4. k_{et}^{-1a} for Complexes **2** and **4** in CH_3CN

	temperature/ $^\circ\text{C}$				
	25	-20	-30	-40	-50
2	0.61	0.60	0.56	0.53	0.50
4	1.20	1.11	0.92	0.56	0.56

^a Values of k_{et}^{-1} are given in units of ps. Uncertainties are 0.02 ps.

and **4** summarize simulated electron-transfer rates for **1**, **2**, and **4** as a function of temperature, up to the freezing point, in methylene chloride and acetonitrile, respectively.

The mixed valence complexes **1–4** show slower k_{et} 's in "slower" solvents, i.e., those with longer t_{1e} 's. How then does freezing the solvent produce faster k_{et} 's? Freezing the solvent

(20) Londergan, C. H.; Rocha, R. C.; Brown, M. G.; Shreve, A. P.; Kubiak, C. P. *J. Am. Chem. Soc.* **2003**, *125* (46), 13912–13913.

(21) Chen, P.; Meyer, T. J. *Inorg. Chem.* **1996**, *35* (19), 5520–5524.

causes the dynamic solvent modes to decouple from very fast ET. Once the dependence on solvent dipole reorientation is lifted, faster internal modes dominate, k_{et} increases as a result, and we expect the $\nu(\text{CO})$ bandshapes to reflect this increase in the ET rate. Examination of Figures 8 and 9 shows that the spectra of complex **4** are indeed more coalesced following freezing of the solvents. Because the time scale of freezing solvent molecules is much slower than that of ET, the mixed valence ions must exist in “averaged” solvent environments upon freezing. This is how valence trapping is avoided at low temperatures.

It is worth commenting on one further ramification of freezing the solvent. Examination of Figures 8 and 9 shows that the coalesced band shapes once the solvent is frozen are nearly identical. This, in turn, means that the rates of electron transfer must be similar for **4** in both solvents *once they are frozen*. This is a striking feature of these figures, especially since the band shapes (and electron-transfer rates) are very different when the solvents are fluid. This is consistent with removal of solvent dynamical terms from ν_N upon freezing the solvent, leaving only the internal vibrational modes of the molecule. Thus, the freezing of both methylene chloride and acetonitrile has the effect of equalizing the ν_N term for these solvents. Because the exponential term is nearly unity for these complexes, we then see that freezing of the solvents must produce nearly identical electron-transfer rates in different solvents. This is verified by the spectra in Figures 8 and 9.

One possible complication of estimating electron exchange rate constants by simulating IR bandshapes is the intrinsic temperature dependence of the contributing bandshapes. It is well-known that IR bandshapes change with temperature, especially following the freezing of the solvent where locking the solute into a solid matrix can greatly increase the contribution of inhomogeneous broadening.²² Because of this, it is important to determine the contributions of IR bandshapes, independent of electron exchange. In order to rule out effects stemming from changes in temperature and state of the solvent, reference spectra of the Ru_3 monomer, **5**, were taken in the neutral and minus one states in methylene chloride from 25 °C to -190 °C and in acetonitrile from 25 °C to -100 °C. The monomer was used so that neutral and fully reduced clusters could be obtained (the ruthenium dimers are unstable in the fully reduced, -2, state). The peak position and full width at half-maximum values were measured for $\nu(\text{CO})$ bands in CH_2Cl_2 and CH_3CN (see Supporting Information). As the solvent temperature decreased, broadening of all the $\nu(\text{CO})$ bands was observed, accompanied by a shift in the peak position. In all cases the shift in peak position was less than 6 cm^{-1} from the starting value over the temperature range investigated. Neither the shift in position nor the changes in the fwhm were sufficient to account for the spectra observed in Figures 8 and 9 (see Supporting Information). This result confirms that the increase in coalescence we have observed in mixed valence ruthenium dimers is due to an increase in the rate of dynamic electron exchange, not the intrinsic temperature dependence of IR bandshapes.

4. Conclusions

IR spectral analysis has been used to probe the effects of solvent upon the rates of electron transfer in mixed valence

systems which are at the Class II–III borderline. We have demonstrated that exchange rates for intramolecular transfer reactions in **1–4** show a strong solvent dependence. The influence that the solvent exerts on the ET rate stems not from static thermodynamic parameters but from parameters of the solvent that figure importantly into its dynamics. In particular, inertial parameters and solvent dipolar reorientation times reported by Maroncelli and co-workers provide strong correlations with the observed electron-transfer rates in the solvents studied.

Building upon this, we have also shown that the solvent dynamics may be decoupled from the electron-transfer event in mixed valence systems through freezing of the solvent. This decoupling removes the solvent dynamical term from the frequency factor, ν_N , in eq 1. Removal of the solvent dynamic contributions leaves only the faster internal modes of the molecule. As such, the electron-transfer rate increases, observable as an increase in the coalescence of the $\nu(\text{CO})$ bands. This behavior further supports the theoretical model that the dynamics of the solvent are controlling the electron-transfer rate in the dimers reported in this study.

In light of the results described here, we believe that a refinement of the defining characteristics of borderline Class II–III mixed valence complexes is in order. We propose that this definition be based upon the influence that the solvent exerts over the mixed valence system. Thus, class II mixed valence ions are defined as those for which the solvent's time independent parameters (i.e., λ_o) are able to fully capture the system's solvent dependence. Class II–III mixed valence ions are those for which the time-independent solvent parameters fail to account for the solvent dependence of the system, but time-dependent parameters (i.e., solvent relaxation times and moments of inertia) are able to capture the solvent dependence of the system. Class III systems are those that are solvent independent with respect to the mixed valence properties (i.e., they show no dependence on either the time-independent or time-dependent properties of the solvent). We believe that these new definitions provide a more accurate description of class II, II–III, and III as well as provide clearer criteria for experimentalists to use when attempting to classify mixed valence systems of interest. This is especially true in the case of large metal complexes where the dynamics of the solvent are much more homogeneous than the dynamics of vibrational modes of the complex, which can easily stretch over several orders of magnitude ($\sim 10^{12} \text{ s}^{-1}$ to $\sim 10^{15} \text{ s}^{-1}$), raising questions concerning the correct time scale to employ for discussions of electronic delocalization.

Acknowledgment. We gratefully acknowledge support from NSF CHE-0616279. We would like to thank Prof. Tasuku Ito for many helpful discussions.

Supporting Information Available: The peak position and full width at half-maximum values for $\nu(\text{CO})$ bands of **5** and **5⁻** in CH_2Cl_2 and CH_3CN . This material is available free of charge via the Internet at <http://pubs.acs.org>.

JA072653M

(22) Turner, J. J. *Handbook of Vibrational Spectroscopy*; John Wiley and Sons Ltd.: 2002; Vol. 1, pp 101–127.